

# Shaping bipolar Planetary Nebulae : How mass loss leads to waistline development.

C. Dijkstra & A. K. Speck

*Department of Physics and Astronomy, University of Missouri, Columbia, MO 65211, USA*

dijkstrac@missouri.edu

## ABSTRACT

Asymptotic Giant Branch (AGB) stars generally have spherically symmetric envelopes, whereas most post-AGB stars and Planetary Nebulae (PNe) show axisymmetric circumstellar envelopes. While various mechanisms for axisymmetric circumstellar structures may explain the shapes of PNe, they do not address how the shape of the circumstellar shell evolves. Here we address the temporal changes in the axisymmetry of AGB star envelopes, and in particular the development of the torus required in the Generalized Interacting Stellar Winds (GISW) model. Assuming (1) an AGB star rotates with sufficient angular speed at the start of the AGB phase; and (2) that the rotational angular momentum of the AGB star is conserved, we demonstrate that some very important observational features of AGB star axisymmetry evolution can be reproduced. We find that, compared to the star's increasing luminosity and decreasing effective temperature, the decreasing mass of the star primarily affects the axisymmetry of the envelope. When a representative mass loss history is adopted, where most of the mass is lost near the end of the AGB phase, the envelope's axisymmetry increases over time, with the strongest increase occurring near the end of the AGB phase. This may naturally explain why most AGB stars have spherically symmetric envelopes, while axisymmetry seems common-place in the post-AGB/PNe phase. The degree of axisymmetry at the end of the AGB phase is found to increase with increasing main sequence mass, and the onset of axisymmetry occurs only after the onset of the superwind (SW) phase, in good agreement with the observations.

*Subject headings:* stars: AGB and post-AGB — stars: circumstellar matter — stars — evolution — stars: late-type — stars: mass loss — stars: winds, outflows

## 1. Introduction

Asymptotic Giant Branch (AGB) stars are the highly evolved descendants of  $1 \lesssim M \lesssim 8 M_{\odot}$  main-sequence stars (Iben & Renzini 1983), which lose mass at a high rate ( $10^{-7}$  to  $10^{-4} M_{\odot}/\text{yr}$ ; see e.g. Habing 1996; Habing and Olofsson 2004). The outflowing matter creates a dusty molecular circumstellar envelope which may completely obscure the central star. As the dust is driven outwards by radiation pressure of the central star, it drags the molecules in the envelope along with it. It is believed that mass-loss rate increases significantly only towards the end of the AGB phase (e.g. Vassiliadis and Wood 1993; Villaver et al. 2002a). This increase in mass-loss rate is necessary to explain the densities seen in typical Planetary Nebulae (PNe; Renzini 1981). The sudden and rapid increase in mass loss has been dubbed the *superwind* (SW; Renzini 1981). Since the invocation of the superwind, many observations of AGB stars have supported this hypothesis (e.g. Knapp & Morris 1985; Wood et al. 1992). During the SW phase the mass-loss rate,  $\dot{M}$ , exceeds  $\dot{M}_{\text{SW}} \approx 10^{-5} M_{\odot}/\text{yr}$  (e.g. Renzini 1981; Wood et al. 1992; Groenewegen and Marigo 2004). After the SW phase AGB stars enter the post-AGB phase, or pre-planetary nebula (PPN) phase, via which they may eventually evolve into PNe. During the post-AGB/PN phase heavy mass loss stops, and the envelope moves away from the star. Meanwhile, the central star heats up and ionizes the circumstellar gas. The remains of the envelope eventually disperse into the Interstellar Medium (ISM), while the central star cools off as a white dwarf (WD).

AGB star evolution is intimately linked to its dust production. The circumstellar dust drives mass loss and shapes the circumstellar environments. While AGB stars generally have spherically symmetric mass loss (e.g. Olofsson 2004), most post-AGB stars and PNe show axisymmetric circumstellar envelopes (Meixner et al. 1999; Waelkens and Waters 2004; Sahai 2004; Soker and Subag 2005). The axisymmetry is seen as a bipolar or hourglass-shaped reflection nebula, where the two lobes (bubbles, jets) of the nebula are separated by an equatorial waist, or torus. The onset of the axisymmetry is believed to occur very near the end of the AGB phase (e.g. Olofsson 2004; Waelkens and Waters 2004). While some PNe are indeed spherical (Soker and Subag 2005), these appear to be old nebulae, and it is increasingly evident that the majority of PNe are aspherical, and that most are bipolar (Soker and Subag 2005).

A suggested mechanism for shaping PNe is the Generalized Interacting Stellar Winds (GISW) model (e.g. Kwok 1982; Kahn and West 1985). In this model a circumstellar torus is present in the equatorial plane of the AGB star. The exact origin of the torus is not specified, but is agreed to be somehow created by the slowly expanding AGB wind. Later, during the post-AGB and PNe phase, a faster wind interacts with this torus. The fast wind is blocked by the torus in the equatorial plane of the AGB star, but may easily flow into the

polar regions, creating a bipolar (P)PN.

The development of axisymmetry, and in particular the origin of the equatorial torus needed to create it in the GISW model, has been attributed to various mechanisms. Here, the presence of a companion star, fast rotating AGB stars, magnetic fields, and the compression of gas into the equatorial region by two jets have been considered in various ways. We will briefly discuss these mechanisms below.

A companion star may have several effects. First, it may cause the AGB star to spin-up (e.g. Harpaz and Soker 1994; Soker and Harpaz 2000). This spin-up may lead to small deviations from spherical symmetry of the AGB star itself, which are subsequently amplified in the dust condensation region due to the non-linear behavior and the strong temperature and density dependence of the dust formation process (Dorfi and Höfner 1996). This then leads to preferential mass loss along the equator. Second, to spin-up an AGB star, the companion must be close (see Sect. 2.3 for a quantification of the necessary proximity). If the companion is close however, and the AGB star’s mass loss rate is high enough, the companion may accrete mass and create jets in the process. This also leads to axisymmetry (Soker 2005, and references therein). Finally, the gravitational influence of a companion star may help shape the AGB star’s envelope into an axisymmetric geometry (Mastrodemos and Morris 1998, 1999).

Several AGB stars and PNe show magnetic fields in their circumstellar environments, and these fields are often suggested to be the main agent responsible for creating axisymmetry. However, Soker (2006) argues that a single star can not supply the energy and angular momentum to create the large coherent magnetic fields required for shaping the circumstellar wind, although magnetic fields may have a secondary role.

Equatorially enhanced densities are commonly attributed to the equatorially-enhanced mass loss of an AGB star. However, they may also originate from the compression of gas into the equatorial region by bipolar jets. Soker and Rappaport (2000) argue that the interaction of a slow AGB wind with a collimated fast wind (CFW) blown by a main-sequence or white dwarf companion leads to equatorial density enhancements. Here, the CFW originates from the accretion of the AGB wind into a disk around the companion. The CFW forms two jets (lobes) along the symmetry axis which compress the slow AGB wind near the equatorial plane, leading to the formation of a dense slowly expanding ring. Later, after the CFW and slow AGB wind cease, the primary star leaves the AGB and blows a second, more spherical, fast wind. This wind is then collimated by the dense equatorial material and leads to a bipolar PN as described by the GISW model.

While these various mechanisms for axisymmetric circumstellar structures may explain

the shapes of PNe, they do not address the time evolution of the shape of the circumstellar shell. In particular, they generally fail to address the fact that most AGB shells are spherical (and remain that way for most of the AGB phase), whereas most post-AGB objects (and PNe) are bipolar (or multi-polar).

In this paper we address the temporal changes in the axisymmetry of the circumstellar envelope, and in particular the development of the torus that is required in the GISW model. For this purpose we consider the scenario of an AGB star that rotates at a sufficient angular speed at the start of the AGB phase. Next, as the star evolves, we assume that the rotational angular momentum of the AGB star is somehow conserved. Although simplistic, we will demonstrate that if the above conditions are met, some very important observational features of AGB star axisymmetry evolution may be reproduced. In Sect. 2 we discuss our model and the validity of its underlying assumptions. In Sect. 3 we discuss the results of the model. Sect. 4 lists our conclusions.

## 2. Model description

We note that in order for what follows to succeed, the AGB star needs to have a sufficiently large angular velocity at the start of the AGB phase. This probably necessitates some sort of a spin-up, which will be discussed in Sect. 3.2.

The mass-loss rate is affected by the escape velocity. A rotating sphere will tend to become oblate and will have a reduced gravitational acceleration,  $g$ , at the equator compared to the pole. With a lower  $g$ , the escape velocity is reduced and thus mass loss increases. Therefore we need to consider the effect this will have on the structure/shape of the circumstellar shell and how this effect changes with time.

### 2.1. Effective gravity ratio between the equator and poles

We start by considering  $\alpha$ , which measures the ratio in effective gravity between the equator and poles of a rotating AGB star. For a test-mass  $m$  at the surface of the star, it is given by

$$\alpha = \frac{GMm/R^2 - m\omega^2 R}{GMm/R^2} = 1 - \frac{\omega^2 R^3}{GM} \quad (1)$$

where  $G$  is the gravitational constant, and  $M$  and  $R$  are the mass and radius of the star.  $\omega$  represents the angular velocity of the star at the equator. We next assume that the angular

momentum of the AGB star is conserved, i.e.

$$I\omega = I_i\omega_i \quad (2)$$

where  $I$  represents the moment of inertia of the star. Here, we adopt the notation that  $x_i$  indicates the initial value of a given quantity  $x$ , i.e. the value of  $x$  right after the spin-up. Assuming solid-body rotation through the stellar envelope, and that at all times the star's deviation from spherical symmetry is small, and ignoring the core's moment of inertia and increasing mass during AGB evolution, we have  $I \propto M_{\text{env}} R^2$ , where  $M_{\text{env}}$  is the envelope's mass. From this it then follows that

$$\omega^2 = \omega_i^2 \left( \frac{M_{\text{env},i}}{M_{\text{env}}} \right)^2 \left( \frac{R_i}{R} \right)^4 \quad (3)$$

Using Eq. 3 and

$$R = R_i \sqrt{\frac{L}{L_i}} \left( \frac{T_{\text{eff},i}}{T_{\text{eff}}} \right)^2 \quad (4)$$

where  $L$  and  $T_{\text{eff}}$  are the luminosity and effective temperature of the star, we then find for  $\alpha$

$$\begin{aligned} \alpha &= 1 - \frac{\omega_i^2 R_i^3}{GM} \left( \frac{M_{\text{env},i}}{M_{\text{env}}} \right)^2 \sqrt{\frac{L_i}{L}} \left( \frac{T_{\text{eff}}}{T_{\text{eff},i}} \right)^2 \\ &= 1 - \frac{\omega_i^2 R_i^3}{GM} \left( \frac{M_i - M_c}{M - M_c} \right)^2 \sqrt{\frac{L_i}{L}} \left( \frac{T_{\text{eff}}}{T_{\text{eff},i}} \right)^2 \quad (5) \end{aligned}$$

where  $M_c$  is the core mass of the star.

Using Eq. 5, we may follow  $\alpha$  as a function of stellar evolution. Since the AGB star's deviations from spherical symmetry are amplified in the dust condensation region (Dorfi and Höfner 1996), the behavior of the degree of axisymmetry in the envelope may in principle be followed as a function of stellar evolution as well.

## 2.2. Axisymmetry of the envelope

The ratio  $\rho_e/\rho_p$ , where  $\rho_e$  and  $\rho_p$  represent the mass density distribution in the equatorial and polar direction respectively, is a measure for the degree of axisymmetry in the envelope. If the exact relation between  $\rho_e/\rho_p$  and  $\alpha$  is known, and if we assume that  $\rho_e/\rho_p$  in first order only depends on  $\alpha$  (see below), we may monitor  $\rho_e/\rho_p$  with stellar evolution.

While the relationship between  $\rho_e/\rho_p$  and  $\alpha$  is non-trivial, we can still make an estimate for such a relation. Dorfi and Höfner (1996) modeled the structure of a stationary dust

driven wind for a  $1 M_{\odot}$  AGB star ( $T_{\text{eff}} = 2600 \text{ K}$ ,  $L = 1.0 \times 10^4 L_{\odot}$  and  $1.2 \times 10^4 L_{\odot}$ ) spun-up by a companion star to various angular velocities, up to  $2 \times 10^{-8} \text{ s}^{-1}$  ( $10^{-8} \text{ s}^{-1}$ ) for the  $1.0 \times 10^4 L_{\odot}$  ( $1.2 \times 10^4 L_{\odot}$ ) star. Here, the spin-up leads to small deviations from spherical symmetry of the AGB star itself, which are subsequently amplified in the dust condensation region due to the non-linear behavior and the strong temperature and density dependence of the dust formation process. The result is an axisymmetric envelope. The models of Dorfi and Höfner (1996) provide rotationally-modulated solutions for the structure of stationary dust-driven winds, both as a function of rotation rate and polar angle. The output of their models includes  $\dot{M}_e/\dot{M}_p$  and  $v_e/v_p$ , the mass-loss rate ratio and terminal outflow-velocity ratio between the equatorial and polar direction.

Using Eq. 1 and  $\rho_e/\rho_p = (\dot{M}_e/\dot{M}_p)/(v_e/v_p)$  we calculated  $\alpha$  and  $\rho_e/\rho_p$  for these models, in order to estimate a relation between them. The result is shown in Fig. 1. As expected, it can be seen that with decreasing  $\alpha$ , i.e. stronger deviations from spherical symmetry of the AGB star,  $\rho_e/\rho_p$  increases, i.e. the envelope becomes more axisymmetric. In the remainder of this paper we will assume that this relation is valid for all AGB stars. The validity of this assumption will be discussed below.

### 2.3. Validity of assumptions

We now briefly discuss the validity of the assumption of conservation of angular momentum of the star, and the assumption of the use of the relation between  $\alpha$  and  $\rho_e/\rho_p$  found in Fig. 1 for all AGB stars.

The most important assumption in our model is that after the spin-up, the rotational angular momentum of the AGB star is conserved. The validity of this assumption is uncertain, since there are various possible sinks and sources of angular momentum for the star. Angular momentum will be lost from the star through its stellar wind (e.g. Soker and Harpaz 2000). This loss can be substantial, and may in principle remove all of the star's angular momentum. Ignoring the magnetic influence beyond the stellar surface and the moment of inertia of the core relative to that of the envelope, and assuming solid body rotation through the envelope, Soker and Harpaz (2000) showed that the amount of angular momentum in the envelope is proportional to  $J_{\text{env}} \propto M_{\text{env}}^{\delta}$ , where  $\delta$  is a constant. For the upper AGB  $\delta = 3$ . Using the initial-final mass relation (Weidemann 2000), which links the main sequence mass of a low or intermediate mass star with its final mass after the AGB phase (i.e. its WD mass), and assuming that the AGB phase terminates when the stellar envelope's mass has been reduced to about  $0.01 M_{\odot}$  (e.g. Bloeker 1995), it can be shown that the envelope mass of a  $1 M_{\odot}$  ( $7 M_{\odot}$ ) changes by a factor  $M_{\text{env},i}/M_{\text{env}} = 45$  (598), i.e. the angular momentum of

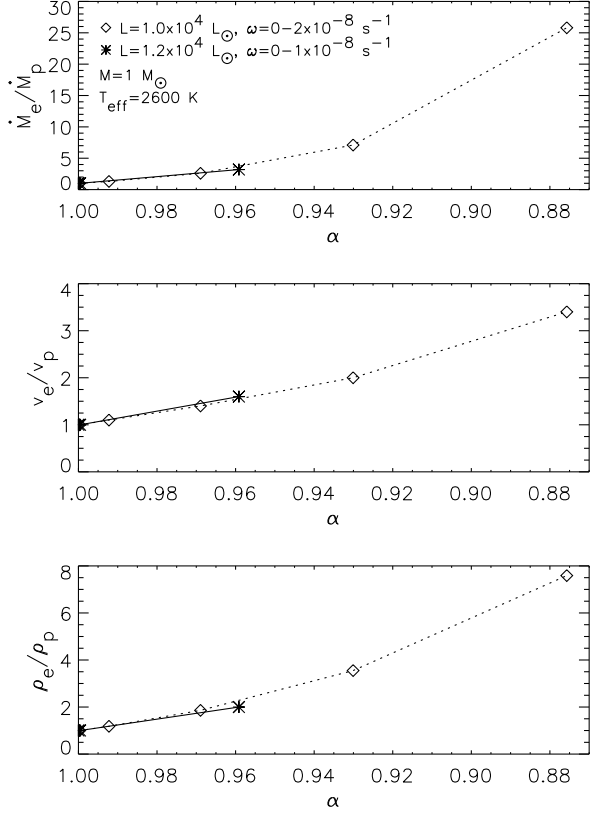


Fig. 1.—  $\dot{M}_e/\dot{M}_p$  (top),  $v_e/v_p$  (middle), and  $\rho_e/\rho_p$  (bottom) as a function of  $\alpha$ . The curves were calculated from detailed model results by Dorfi and Höfner (1996). The calculations were done for a  $1 M_\odot$ ,  $T_{\text{eff}} = 2600 \text{ K}$ , AGB star for two different luminosities (for a  $1.0 \times 10^4 L_\odot$  star, rotating up to  $2 \times 10^{-8} \text{ s}^{-1}$ , and a  $1.2 \times 10^4 L_\odot$  star, rotating up to  $10^{-8} \text{ s}^{-1}$ ). For details see the main text.

the star decreases by a factor  $J_{\text{env},i}/J_{\text{env}} \approx 9 \times 10^4 (2 \times 10^8)!$  The loss of angular momentum through the stellar wind is therefore important. Other means by which the envelope may lose angular momentum include magnetic breaking and expansion of the convective envelope on the AGB (Heger and Langer 1998).

Sources of angular momentum for the envelope may be provided by companion stars/planets and the core of the star. First, at the expense of its orbital angular momentum, a low mass companion may feed angular momentum to the envelope during a common envelope phase (e.g. Harpaz and Soker 1994; Soker and Harpaz 2000). The angular momentum of a com-

panion of mass  $M_p$  is given by (Soker and Harpaz 2000)

$$J_p = 8 \times 10^{49} \left( \frac{M_p}{M_J} \right) \sqrt{\frac{M_i}{0.9 M_\odot} \frac{a}{1 \text{ AU}}} \text{ g cm}^2 \text{ s}^{-1}, \quad (6)$$

where  $M_J$  is Jupiter’s mass and  $a$  is the initial orbital separation. Following Soker and Harpaz (2000), we may express the envelope’s angular momentum as

$$\begin{aligned} J_{\text{env}} &= I\omega \\ &= \gamma M_{\text{env}} R^2 \omega \\ &\approx 2 \times 10^{52} \left( \frac{\gamma}{2/9} \right) \left( \frac{M_{\text{env}}}{1 M_\odot} \right) \times \\ &\quad \left( \frac{R}{1 \text{ AU}} \right)^2 \left( \frac{\omega}{10^{-8} \text{ s}^{-1}} \right) \text{ g cm}^2 \text{ s}^{-1} \quad , \end{aligned} \quad (7)$$

where  $\gamma$  is a constant ( $\gamma = 2/9$  is appropriate for the upper AGB). Comparing Eq. 6 and Eq. 7 shows that e.g. a  $M_p \approx 100 M_J = 0.1 M_\odot$  companion star with an initial orbital separation of 1 AU may replace all of the rotational angular momentum lost by the envelope of a star with  $M_i = 1 M_\odot$ ,  $M_{\text{env}} \leq 0.45 M_\odot$ ,  $R = 1 \text{ AU}$ , and  $\omega = 10^{-8} \text{ s}^{-1}$ . Likewise, a  $M_p \approx 500 M_J = 0.5 M_\odot$  companion star with an initial orbital separation of 1 AU may replace all of the rotational angular momentum lost by the envelope of a star with  $M_i = 7 M_\odot$ ,  $M_{\text{env}} \leq 5.98 M_\odot$ ,  $R = 1 \text{ AU}$ , and  $\omega = 10^{-8} \text{ s}^{-1}$ . The above illustrates that (a substantial fraction of) the angular momentum lost by the wind can in principle be replaced by a low mass companion star.

Second, García-Segura et al. (1999) argue that although the envelope of low- and intermediate-mass stars may be devoid of angular momentum (i.e. non-rotating) at the beginning of the thermally pulsing AGB phase, stars with main sequence masses  $\gtrsim 1.3 M_\odot$  can spin up their envelopes to rotational speeds of  $\sim 1 \text{ km/s}$  just prior to the PN ejection. Here, the spin-up is caused by angular momentum from the core that *leaks* to the envelope during thermal pulses (García-Segura et al. 1999).

The validity of our assumption of angular momentum conservation for the star thus remains to be seen. However, as we will demonstrate in the following section, if this condition is somehow met, some very important observational features of AGB stars may be reproduced. It is therefore interesting to consider the scenario where the star’s angular momentum is conserved, despite the uncertainty of this assumption.

Strictly speaking, the relationship found between  $\rho_e/\rho_p$  and  $\alpha$  (see Fig. 1, lower panel) is of course only valid for the  $1 M_\odot$  AGB star modeled above. Still, it may not be unreasonable to assume that  $\rho_e/\rho_p$  will in first order primarily depend on  $\alpha$ , since it is the deviation from



axisymmetry of the AGB star that leads to an axisymmetric envelope in the first place. If this assumption is correct, we may apply the obtained relationship to other stars as well, and generally study  $\rho_e/\rho_p$  as a function of stellar parameters and evolution (see below). If the assumption is invalid, the behavior of  $\alpha$  still provides information on the general behavior of  $\rho_e/\rho_p$  for a given star, since deviations from spherical symmetry of the AGB star will still be amplified in the dust condensation region (Dorfi and Höfner 1996). Only the exact relation between  $\alpha$  and  $\rho_e/\rho_p$  may not be specified in this case.

### 3. Results of the model

#### 3.1. Axisymmetry and stellar parameters

As AGB stars evolve, their luminosity increases, while their mass and effective temperature decrease. Following Eq. 5, the effect of  $L$  and  $T_{\text{eff}}$  is thus to increase  $\alpha$  (i.e. lower the degree of axisymmetry) over time, while the effect of  $M$  will be to decrease  $\alpha$  (i.e. increase the degree of axisymmetry) over time. Here, the stellar mass has the largest effect on  $\alpha$  and hence the axisymmetry in the envelope. While the luminosity of the star typically increases by a factor of 10 during AGB star evolution,  $\alpha$  (see Eq. 5) depends on  $\sqrt{L_i/L}$ , which only decreases by a factor of 3. Likewise, while  $\alpha$  depends on  $(T_{\text{eff}}/T_{\text{eff},i})^2$ , the effective temperature typically decreases from 3500 K to 2500 K, so  $(T_{\text{eff}}/T_{\text{eff},i})^{-2}$  decreases at most by a factor 2. In contrast,  $\alpha$  varies with the stellar mass as  $(1/M)((M_i - M_c)/(M - M_c))$ . Assuming its tip of the AGB envelope mass is  $\sim 0.01 M_\odot$  (Blöcker 1995),  $\alpha$  may therefore vary by a factor of about  $3.6 \times 10^3$  ( $2.5 \times 10^6$ ) over the lifetime of a  $1 M_\odot$  ( $7 M_\odot$ ) star. The axisymmetry in the envelope will thus indeed be primarily affected by the stellar mass.

#### 3.2. Axisymmetry and stellar evolution

We now investigate the time evolution of  $\rho_e/\rho_p$  under the influence of mass loss during the AGB phase. This is shown in Fig. 2 for four stars with different main sequence masses. It is assumed that each star is spun-up to an initial rotational velocity of 0.076 km/s. This choice of initial rotational velocity ensures that, when combined with the other stellar parameters adopted for each star,  $\alpha$  is always in the range covered by the models of Dorfi and Höfner (1996), therefore allowing a translation to  $\rho_e/\rho_p$  to be made. After the spin-up each star has an initial luminosity of  $3000 L_\odot$ , an initial effective temperature of 3500 K, an initial radius of  $\sim 0.7$  AU, and an initial mass loss rate of  $\dot{M}_i = 10^{-7} M_\odot/\text{yr}$ . After spin-up, the

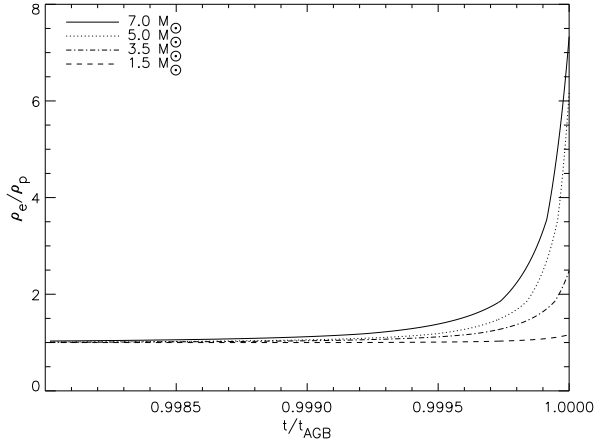


Fig. 2.—  $\rho_e/\rho_p$  as a function of time for stars with initial masses of  $1.5 M_\odot$  (*dashed*),  $3.5 M_\odot$  (*dashed dotted*),  $5.0 M_\odot$  (*dotted*), and  $7.0 M_\odot$  (*solid*). For details see the main text.

stars lose mass according to

$$\dot{M}(t) = \dot{M}_i \times \exp \left( \left( \frac{t}{t_{\text{AGB}}} \right)^n \ln \left( \frac{\dot{M}_f}{\dot{M}_i} \right) \right) , \quad (8)$$

where  $\dot{M}_f$  is the final mass loss rate, and the time  $t$  is expressed in terms of the total AGB lifetime,  $t_{\text{AGB}}$ . The parameter  $n$  may be found by specifying the onset of the SW phase,  $t_{\text{SW}}$ , which is also expressed in terms of  $t_{\text{AGB}}$ . Here we use

$$n = \frac{\ln(\ln(\frac{\dot{M}_{\text{SW}}}{\dot{M}_i}) / \ln(\frac{\dot{M}_f}{\dot{M}_i}))}{\ln(\frac{t_{\text{SW}}}{t_{\text{AGB}}})} , \quad (9)$$

where  $t_{\text{SW}}$  is estimated from detailed model results by Vassiliadis and Wood (1993), and  $t_{\text{AGB}}$  and  $\dot{M}_f$  are adjusted such that the initial-final mass relation (Weidemann 2000) is satisfied for each star. Then the mass of the star is found by

$$M(t) = M_i - \int_0^t \dot{M}(t') dt' . \quad (10)$$

The exact mass-loss rate as a function of time during the AGB phase is unknown and difficult to determine. Still, a key feature of it seems to be that most of the mass is lost near the end of the AGB phase (e.g. Renzini 1981; Vassiliadis and Wood 1993). With our choice of  $\dot{M}(t)$  this condition is satisfied. We may now insert Eq. 10 into Eq. 5 to follow  $\alpha$  as a function of time. Next, we use the results of Fig. 1 to translate  $\alpha$  into  $\rho_e/\rho_p$ , yielding the results shown in Fig. 2. Note that we kept  $L$  and  $T_{\text{eff}}$  constant at  $L = 1 \times 10^4 L_\odot$  and  $T_{\text{eff}} = 2500 \text{ K}$  in the

Table 1: Model parameters for the stars shown in Fig. 2.  $\Delta t_{\text{AX},2}$  and  $\Delta t_{\text{AX},5}$  represent the time before the end of the AGB phase in which  $\rho_e/\rho_p$  exceeds 2 and 5 respectively, i.e. when a reasonable axisymmetry may be observed in our model calculations. The symbol – is used when no value for  $\Delta t_{\text{AX},2}$  or  $\Delta t_{\text{AX},5}$  is available. For an explanation of the other parameters see the main text.

$M_i$ ( $M_\odot$ )	$L_i$ ( $L_\odot$ )	$L$ ( $L_\odot$ )	$T_{\text{eff},i}$ (K)	$T_{\text{eff}}$ (K)	$R_i$ (AU)	$v_i$ (km/s)	$\dot{M}_i$ ( $M_\odot/\text{yr}$ )	$\dot{M}_{\text{SW}}$ ( $M_\odot/\text{yr}$ )	$\dot{M}_f$ ( $M_\odot/\text{yr}$ )	$t_{\text{AGB}}$ (yr)	$t_{\text{SW}}^\dagger$ ( $t_{\text{AGB}}$ )	$\Delta t_{\text{AX},2}$ (yr)	$\Delta t_{\text{AX},5}$ (yr)
1.5	3000	10000	3500	2500	0.7	0.076	$1.0 \times 10^{-7}$	$1.0 \times 10^{-5}$	$3.0 \times 10^{-5}$	$2.3 \times 10^6$	0.99	–	–
3.5	3000	10000	3500	2500	0.7	0.076	$1.0 \times 10^{-7}$	$1.0 \times 10^{-5}$	$3.0 \times 10^{-5}$	$2.1 \times 10^6$	0.96	82	–
5.0	3000	10000	3500	2500	0.7	0.076	$1.0 \times 10^{-7}$	$1.0 \times 10^{-5}$	$5.5 \times 10^{-5}$	$1.4 \times 10^6$	0.92	202	23
7.0	3000	10000	3500	2500	0.7	0.076	$1.0 \times 10^{-7}$	$1.0 \times 10^{-5}$	$1.0 \times 10^{-4}$	$6.9 \times 10^5$	0.80	162	30

<sup>†</sup>Values estimated from detailed models results by Vassiliadis and Wood (1993).

above analysis (where  $L$  and  $T_{\text{eff}}$  are not to be confused with  $L_i$  and  $T_{\text{eff},i}$ ). As discussed earlier, the effect of  $L$  and  $T_{\text{eff}}$  are minor compared to the effects of the stellar mass. These adopted values for  $L$  and  $T_{\text{eff}}$  ensure that the derived values for  $\rho_e/\rho_p$  are in fact lower limits. Table 1 lists the parameters adopted for each model in Fig. 2.

Fig. 2 shows that the axisymmetry increases over time. Here, the strongest increase is clearly only near the very end of the AGB phase, which is due to the fact that the star loses most of its mass only at this stage (Vassiliadis and Wood 1993; Villaver et al. 2002a). This result may naturally explain why most AGB stars have spherically symmetric envelopes, while in the post-AGB/PNe phase axisymmetry seems common-place (Meixner et al. 1999; Waelkens and Waters 2004; Sahai 2004; Soker and Subag 2005).

Fig. 2 also shows that the final degree of axisymmetry, i.e. the degree of axisymmetry at the end of the AGB, increases with increasing main sequence mass. This result also seems to agree with observations. Indeed, an optical imaging survey of post-AGB stars by Ueta et al. (2000) with the Hubble Space Telescope (HST) seems to suggest that higher mass progenitor AGB stars are more likely to show bipolar structure with a completely or partially obscured central star than low mass stars. This result seems to be reinforced by detailed radiative transfer calculations of Meixner et al. (2002) for the post-AGB stars HD 161796 and IRAS 17150-3224.

It is interesting to note that the onset of axisymmetry does not coincide with the onset of the SW phase. This is illustrated in Fig. 2 and Table 1. The onset of axisymmetry only

becomes reasonably apparent (i.e.  $\rho_e/\rho_p \gtrsim 2$ ) in the last few tens or hundreds of years, long after the start of the SW phase. This is in agreement with e.g. recent findings by Ueta (2006). Based on Spitzer Space Telescope (SST; Werner et al. 2004) observations of NGC 650 (Program ID 77), Ueta (2006) shows that mass loss is nearly isotropic when the SW is turned on towards the end of the AGB phase, and the SW mass loss precipitously decreases along the polar direction during the SW phase.

The degree of axisymmetry that develops in the envelope will strongly depend on the initial rotational velocity of the AGB star. Generally, the rotation of single stars is expected to slow down significantly while they are on the main-sequence (e.g. García-Segura et al. 1999; Soker 2006), and once these stars reach the AGB phase they are believed to rotate too slowly for axisymmetries to develop (Dorfi and Höfner 1996). Here, slow rotation is expected both with and without the presence of magnetic fields (Soker 2006). It is therefore often argued that a companion star is prerequisite to spin-up an AGB star (e.g. Harpaz and Soker 1994; Soker and Harpaz 2000). The mechanism adopted in this paper would benefit from the presence of such a binary companion, since it may spin-up the AGB star, and be a source of rotational angular momentum for the AGB star’s envelope that is otherwise lost through the AGB wind (see Sect. 2.3). Moreover, the requirement of a companion star would fit in nicely with the idea that binary interaction indeed plays an important role in shaping the axisymmetric structure of PNe (see Sect. 1), and recent observational results that strongly suggest that most or even all PNe are in close binary systems (De Marco et al. 2005).

Alternatively, in case of stars with main sequence masses  $\gtrsim 1.3 M_\odot$ , the spin-up may be provided by angular momentum from the core of the AGB star during thermal pulses (see Sect. 2.3), in which case a companion star is not required. The thermal pulses will not provide the star with a spin-up at the start of the AGB phase, since these pulses only occur late in the AGB phase. However, they may efficiently spin-up the AGB star near the end of the AGB phase (García-Segura et al. 1999), during which the mechanism adopted in our paper may still apply. In this case, it seems more appropriate to use  $M_{\text{env},i} \approx 0.1 M_\odot$ , since at the onset of the thermal pulses the mass of the envelope may already have been substantially reduced down to  $\sim 0.1 M_\odot$  (García-Segura et al. 1999). Here, the lower initial envelope mass will result in a lower degree of axisymmetry in the envelope, since  $\alpha$  (see Eq. 5) will stay closer to unity.

Although the trends described for  $\rho_e/\rho_p$  are in nice agreement with observations, the absolute values predicted for  $\rho_e/\rho_p$  are somewhat low. For example, we predict a final value of  $\rho_e/\rho_p \approx 1.2$  for a  $1.5 M_\odot$  main sequence star. In contrast, for the post-AGB star HD 161796, which is believed to be of a low main sequence mass (e.g. Meixner et al. 2002, and references therein), Meixner et al. (2002) find  $\rho_e/\rho_p \approx 9$ . Also, we predict a final value of  $\rho_e/\rho_p \approx 7.3$

for a  $7.0 M_{\odot}$  main sequence star, which is on the high mass end of AGB stars. Still, Meixner et al. (2002) find for e.g. the high mass post-AGB star IRAS 17150-3224  $\rho_e/\rho_p \approx 160$ , which is clearly much larger than predicted by our models. However, the trend of an increasing value of  $\rho_e/\rho_p$  with increasing main sequence mass is the same.

There may be several reasons for our under-prediction of  $\rho_e/\rho_p$ . First, the assumed initial rotational velocity of 0.076 km/s is rather low. As discussed earlier, this choice ensured that, when combined with the other stellar parameters adopted for our stars,  $\alpha$  is always in the range covered by the models of Dorfi and Höfner (1996), therefore allowing a translation to  $\rho_e/\rho_p$  to be made. This is a computational restriction however, and not a physical one. In fact, rotational velocities higher than we adopted may be expected (see e.g. García-Segura et al. 1999, and references therein). Adopting a higher initial rotational velocity will increase  $\rho_e/\rho_p$ . Also, we have only considered the effects of mass thusfar. Taking properly into account the effects of the luminosity and effective temperature of the star as well may also help increase  $\rho_e/\rho_p$ . For example, we adopted a luminosity of  $L = 1 \times 10^4 L_{\odot}$  for all stars. Still, for stars with low main-sequence masses this luminosity may be too high. Lowering it will help increase  $\rho_e/\rho_p$  in this case. Finally, the values of  $\rho_e/\rho_p$  derived by Meixner et al. (2002) for HD 161796 and IRAS 17150-3224 will depend on the details of their radiative transfer calculations. Possibly, a different assumption of e.g. dust composition or grain size distribution may lower the values of  $\rho_e/\rho_p$  derived by Meixner et al. (2002), in better agreement with our results.

#### 4. Conclusions

In this paper we addressed the temporal changes in the axisymmetry of AGB star envelopes, and in particular the development of the torus that is required in the GISW model. For this purpose we considered the scenario of an AGB star that rotates at a sufficient angular speed at the start of the AGB phase. Next, as the star evolves, we assumed that the rotational angular momentum of the AGB star is somehow conserved. If the above condition is met, some very important observational features of AGB star axisymmetry evolution may be reproduced. In particular compared to the star’s increasing luminosity and decreasing effective temperature, the decreasing mass of the star primarily affects the axisymmetry of the envelope. Adopting a representative mass loss history, where most of the mass is lost near the end of the AGB phase, results in an increase of the envelope’s axisymmetry over time. The strongest increase is only near the very end of the AGB phase, explaining why most AGB stars have spherically symmetric envelopes, while those of post-AGB stars and PNe are axisymmetric. Also, the degree of axisymmetry at the end of the AGB phase is found

to increase with increasing main sequence mass, and the onset of axisymmetry only occurs after the onset of the SW phase. Our findings are in good agreement with observations.

This work was supported by the NASA Astrophysical Data Program (NAG 5-12675) and the University of Missouri Research Board. We are very grateful to Noam Soker for directing our background reading regarding the effects of binaries on the morphology of circumstellar envelopes, and to Adam Frank and Toshiya Ueta for initial feedback. AKS would like to thank her WS06 Stellar Astrophysics class for their indulgence in debating the idea behind this paper during our discussion of stellar evolution.

## REFERENCES

- Blöcker, T. 1995, *A&A*, 297, 727
- Dorfi, E. A. & Höfner, S. 1996, *A&A*, 313, 605
- García-Segura, G., Langer, N., Różyczka, M., & Franco, J. 1999, 517, 767
- Groenewegen, M. A. T., & Marigo, P. 2004, *Asymptotic Giant Branch Stars*, 105
- Habing, H. J. 1996, *A&A Rev.*, 7, 97
- Habing, H. J., & Olofsson, H. 2004, *Asymptotic Giant Branch Stars*, 1
- Harpaz, A., & Soker, N. 1994, *MNRAS*, 270, 734
- Heger, A., & Langer, N. 1998, *A&A*, 334, 210
- Iben, I. Jr., & Renzini, A. 1983, *ARA&A*, 21, 271
- Kahn, F. D., & West, K. A. 1985, *MNRAS*, 212, 837
- Knapp, G. R., & Morris, M. 1982, *ApJ*, 292, 640
- Kwok, S. 1982, *ApJ*, 258, 280
- De Marco, O., Moe, M., Herwig, F., & Politano, M. 2005, *American Astronomical Society Meeting Abstracts*, 207
- Mastrodemos, N., & Morris, M. 1998, *ApJ*, 497, 303
- Mastrodemos, N., & Morris, M. 1999, *ApJ*, 523, 357

- Meixner, M. et al., 1999, *ApJS*, 122, 221
- Meixner, M., Ueta, T., Bobrowsky, M., & Speck, A. 2002, *ApJ*, 571, 936
- Olofsson, H. 2004, *Asymptotic Giant Branch Stars*, 325
- Renzini, A., 1981, *Physical Processes in Red Giants*, eds. I. Iben Jr. & A. Renzini, Reidel:Dordrecht, 431
- Sahai, R. 2004, *ASP Conf. Ser. 313: Asymmetrical Planetary Nebulae III: Winds, Structure and the Thunderbird*, eds. M. Meixner, J. H. Kastner, B. Balick & N. Soker, 141
- Soker, N., & Harpaz, A. 2000, *MNRAS*, 317, 861
- Soker, N., & Rappaport, S. 2000, *ApJ*, 538, 241
- Soker, N. 2005, *AJ*, 129, 947
- Soker, N., & Subag, E. 2005, *AJ*, 130, 2717
- Soker, N. 2006, *PASP*, 118, 260
- Ueta, T., Meixner, M., & Bobrowsky, M. 2000, *ApJ*, 528, 861
- Ueta, T. 2006, *ApJ*, accepted.
- Vassiliadis, E., & Wood, P. R. 1993, *ApJ*, 413, 641
- Villaver, E., Manchado, A., & Garcia-Segura, G., 2002a, *ApJ*, 581, 1204
- Waelkens, C., & Waters, L. B. F. M. 2004, *Asymptotic Giant Branch Stars*, 519
- Weidemann, V. 2000, *A&A*, 363, 647
- Werner, M. W. et al., 2004, *ApJS*, 154, 1
- Wood, P.R., et al. 1992, *ApJ*, 397, 552